Journal of Materials Chemistry C

A Glass-ceramics with Thermally Stable Blue-red emission for High-power Horticultural LEDs Application

Journal:	*Journal of Materials Chemistry C*
Manuscript ID	TC-ART-01-2020-000061
Article Type:	Paper
Date Submitted by the Author:	06-Jan-2020
Complete List of Authors:	Chen, Weibin; south of china agricultural Zhang, Xuejie; South China Agricultural University Guangzhou, CN, College of Materials and Energy zhou, jianxian; South China Agricultural University Zhang, Haoran; Department of Applied Chemistry, College of Science, South China Agricultural University, Yang, Xiang; South China Agricultural University College of Horticulture Xia, Zhiguo; South China University of Technology, School of materials science and engineering Liu, YingLiang; South China Agricultural University, School of Materials and Energy Molokeev, Maxim S. ; Kirensky Institute of Physics SB RAS, Xie, Gening; South China Agricultural University, College of Materials and Energy, South China Agricultural University; South China Agricultural University, Guangdong Laboratory of Lingnan Mordern Agriculture, Guangzhou, 510642, China; South China Agricultural University, Guangdong Provincial Engineering Technology Research Center for Optical Agriculture Lei, Bingfu; South China Agricultural University, Department of Materials Science and Enginggering; South China Agricultural University, College of Horticulture

Journal of Materials Chemistry C
Materials for optical, magnetic and electronic devices

Guidelines for Reviewers

Thank you very much for agreeing to review this manuscript for *Journal of Materials Chemistry C*.

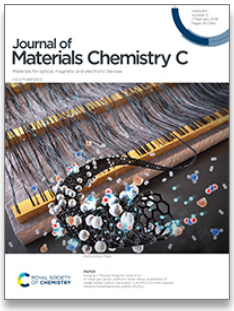

Journal of Materials Chemistry C is a weekly journal in the materials field. The journal is interdisciplinary, publishing work of international significance on all aspects of materials chemistry related to applications in optical, magnetic and electronic devices. Articles cover the fabrication, properties and applications of materials.

Journal of Materials Chemistry C's Impact Factor is **6.641** (2018 Journal Citation Reports®)

The following manuscript has been submitted for consideration as a

FULL PAPER

For acceptance, a Full paper must report primary research that demonstrates significant **novelty and advance**, either in the chemistry used to produce materials or in the properties/ applications of the materials produced. Work submitted that is outside of these criteria will not usually be considered for publication. The materials should also be related to the theme of optical, magnetic and electronic devices.

When preparing your report, please:

- Focus on the **originality**, **importance**, **impact** and **reproducibility** of the science.
- Refer to the **journal scope and expectations**.
- **State clearly** whether you think the article should be accepted or rejected and give detailed comments (with references) both to help the Editor to make a decision on the paper and the authors to improve it.
- **Inform the Editor** if there is a conflict of interest, a significant part of the work you cannot review with confidence or if parts of the work have previously been published.
- **Provide your report rapidly** or inform the Editor if you are unable to do so.

Best regards,

Professor Peter Skabara
Editor-in-Chief
University of Glasgow, UK

Dr Sam Keltie
Executive Editor
Royal Society of Chemistry

Contact us

Please visit our reviewer hub for further details of our processes, policies and reviewer responsibilities as well as guidance on how to review, or click the links below.

What to do when you review

Reviewer responsibilities

Process & policies

Dear Editor of ***Journal of Materials Chemistry C***,

As true readers of ***Journal of Materials Chemistry C*** on a regular basis, we are impressed by its high-quality articles, comprehensive and informative content. Hence, we submitted the manuscript entitled "***A Glass-ceramics with Thermally Stable Blue-red emission for High-power Horticultural LEDs Application***" to ***Journal of Materials Chemistry C*** gladly. Our paper has been prepared in accordance with the regulations of ***Journal of Materials Chemistry C***. The authors are Weibin Chen, Xuejie Zhang, Jianxian Zhou, Haoran Zhang, Xiang Yang, Zhiguo Xia, Yingliang Liu, Maxim S. Molokeev, Gening Xie and Bingfu Lei. The author to whom correspondence should be addressed is Bingfu Lei whom email address is tleibf@scau.edu.cn.

The reasons why we think that publication of our work in ***Journal of Materials Chemistry C*** are as follows:

At present, horticultural light sources are developing rapidly towards the direction of high energy density, high output power and high stability, which poses a challenge to traditional phosphor conversion devices. Focus on this challenge, this work reported that a kind of all-inorganic blue-red dual-emitting light convertor consisting of $Ba_{1.3}Sr_{1.7}MgSi_2O_8:Eu^{2+}$, Mn^{2+} (BSMS) phosphor in glass (PiG) plates were prepared to improve service lifetime and thermal stability. It's equipped with an extern quantum efficiency of 45.3%, an outstanding thermal stability and specific emission spectrum that is highly matched with the absorption of chlorophyll and *β*-carotene. Moreover, a proof-of-concept BSMS-PiG horticultural lamp for application in indoor plant factory was successfully fabricated base on ~370 nm emitting LED chip and the blue-red ratio of spectrum was regulated by controlling the thickness of BSMS-PiG and the concentrations of Mn^{2+} ions in BSMS-PiG. The BSMS-PiG horticultural LEDs were applied in indoor cultivation of Romaine lettuce. The results indicated that biomass of Romaine lettuce was 58.21% greater than those cultivated under the light sources of commercial plant lamps. Besides, the content of total chlorophyll, *β*-carotene and soluble protein were improved. Consequently, the BSMS-PiG horticultural LEDs is a potential candidate for high-power horticultural light source. For the aims of academic intercourse and further developing of the work, we expect that the research might be published in ***Journal of Materials Chemistry C.***

We earnestly hope for your assessment of my paper at your earliest convenience. We look forward to your early reply by sending E-mail message to: tleibf@scau.edu.cn (Bingfu Lei) or by fax (+86-20-85282603).

If our paper causes some problems to you or you have some comments and suggestions, please feel free to contact us.

Thank you very much in advance for your kindly consideration. We are looking forward to hearing from you.

Best wishes

Sincerely your
Bingfu Lei
Jan. 06, 2020

ARTICLE

A Glass-ceramics with Thermally Stable Blue-red emission for High-power Horticultural LEDs Application

Received 00th January 20xx,
Accepted 00th January 20xx

DOI: 10.1039/x0xx00000x

Weibin Chen,[a] Xuejie Zhang,[a] Jianxian Zhou,[a] Haoran Zhang,[a] Xiang Yang,[b] Zhiguo Xia,[c] Yingliang Liu,[a] Maxim S. Molokeev,[d,e] Gening Xie,[a] and Bingfu Lei[a,b,*]

As one of the key elements for indoor agriculture, horticultural light sources are developing rapidly towards high energy density, high output power and high stability, which poses a challenge to traditional phosphor conversion devices. Grasping the nettle, all-inorganic blue-red dual-emitting light convertor consisting of $Ba_{1.3}Sr_{1.7}MgSi_2O_8:Eu^{2+}$, Mn^{2+} (BSMS) phosphor in glass (PiG) plates were prepared to improve duration lifetime for high-power light-emitting diodes (LEDs) and meet the light quality requirements of photosynthesis for indoor agriculture. These obtained samples show an external quantum efficiency of 45.3%, outstanding thermal stability and specific emission spectrum that highly matched with the absorption of chlorophyll and β-carotene. Moreover, a proof-of-concept BSMS-PiG horticultural lamp for application in indoor plant factory was successfully fabricated base on ~370 nm emitting LED chip and the blue-red ratio of its spectrum was regulated by controlling the thickness of BSMS-PiG and the concentrations of Mn^{2+} ions in BSMS-PiG. The BSMS-PiG horticultural LEDs were applied in indoor cultivation of Romaine lettuce. The results indicated that biomass of Romaine lettuce was 58.21% greater than those cultivated under the light sources of commercial plant lamps. Especially, the content of total chlorophyll, β-carotene and soluble protein were improved. The BSMS-PiG horticultural LEDs is a potential candidate for high-power horticultural light source.

1 Introduction

Farmland soil suffered varying degrees of contamination, which has caused a serious threat on food safety, ecological environment and agricultural sustainable development[1,2]. To supply enough food for a rapidly expanding population, agriculture have to be intensified to solve the contradiction between population, resources and environment. Indoor artificial plant factory as a new model of agriculture came into being and achieved greater development[3].

Light energy is the core of plant factory and one of the essential conditions for plant growth and ontogeny. It affects plant metabolism and development in vegetation process[4]. Especially in blue (400−500 nm), red (600−690 nm), and far red (720−740 nm) regions, these energy distribution is accountable to phototropic processes, photosynthesis, and plant photomorphogenesis, respectively[5]. For indoor agriculture, LED is a very promising technology that provides a variety of possibilities for horticultural lighting[6]. Compared with traditional light sources for plant growth such as halogen lamps or high pressure sodium lamp, it has high luminous efficiency, low power consumption, long life and other technical advantages[7]. LEDs have emission peaks ranging from UV-C (~250 nm) to infrared (~1000 nm), and can control specific spectrum composition with light convertor[8]. For this reason, LED lighting technology provides a highly controllable lighting condition to increase productivity and control over horticultural products. In addition, the intensity of light is also a significant factor affecting plant growth[9]. High-intensity illumination is beneficial to secondary metabolic behavior of plants, such as self-repair and active oxygen quenching[10]. This forced horticultural light sources to develop towards the direction of high energy density, high output power and high stability, which poses a challenge to phosphor conversion devices[11,12].

To solve this problem, all-inorganic luminescent glass ceramics were proposed by continuous efforts of researchers, which solved the serious aging problem of traditional fluorescent powder and silicone composite materials with their excellent physical and chemical stability[13,14]. For instance, Chen et al[15] enhanced luminescence of $Y_3Al_5O_{12}:Mn^{4+}$ by impurity doping and fabricated a colour convertor through phosphor-in-glass approach. Wang et al[16] reported a bright red-emitting phosphor $BaMgAl_{10}O_{17}:Mn^{4+}$, Mg^{2+} and embedded the phosphor into an oxide glass matrix to replace phosphor in organic silicone. Deng et al[17] prepared an ultrastable red-emitting glass ceramics by $3.5MgO•0.5MgF_2•GeO_2:Mn^{4+}$

[a] Guangdong Provincial Engineering Technology Research Center for Optical Agriculture, College of Materials and Energy, South China Agricultural University, Guangzhou 510642, P. R. China.
[b] College of Horticulture, South China Agricultural University, Guangzhou 510642, P. R. China.
[c] The State Key Laboratory of Luminescent Materials and Devices, and Guangdong Provincial Key Laboratory of Fiber Laser Materials and Applied Techniques, School of Materials Science and Engineering, South China University of Technology, Guangzhou 510641, P. R. China.
[d] Laboratory of Crystal Physics, Kirensky Institute of Physics, Federal Research Center KSC SB RAS, Krasnoyarsk 660036, Russia.
[e] Siberian Federal University, Krasnoyarsk 660041, Russia
† E-mail: tleibf@scau.edu.cn
Electronic Supplementary Information (ESI) available: [details of any supplementary information available should be included here]. See DOI: 10.1039/x0xx00000x

phosphor in glass matrix for superior high-power artificial plant growth LEDs. Furthermore, Li et al[18] reported that a spliced highly efficient and dual broad emitting light convertor, in which $BaMgAl_{10}O_{17}:Eu^{2+}$ and $CaAlSiN_3:Eu^{2+}$ provide blue and red emission, respectively. However, the above-reported light convertor have many shortcomings. Either the emission peaks in the blue region are too narrow to fully match the absorption spectra of plant photosynthesis[19,20], or the preparation process is complex and excitation light leaks through the patchwork seams[21]. Narrow-band blue-light emitting can't fully meet the physiological needs of plants[22] and the ultraviolet light with coming from the gap of splicing PiG was wasted. To foster the strengths and circumvent the weaknesses, the light converting material should be required with dual-broadband emission and no light leakage, as well as superior stability.

Hence, the choice of fluorescent component is especially important for all-inorganic glass ceramics used on high-power plant lamps. The phosphor $(Ba,Sr)_3MgSi_2O_8$ co-doped with Eu^{2+} and Mn^{2+} has been used for color correction in agricultural lamps because of the intense blue- and red-emission bands[23-25]. Structurally optimized $Ba_{1.3}Sr_{1.7}MgSi_2O_8:Eu^{2+}$, Mn^{2+} possess two emission bands at 430 nm and 660 nm suitable for plant photosynthesis. Mao et al[26] determined its structure and the optimal doping amount of 6% Eu^{2+} ions. It is a very promising material as the fluorescent component of luminescent glass ceramics in monolithic light converting materials. For high-power LEDs, phosphor devices must have excellent thermal stability to withstand the heat emitted by LED chips. At present, the $Ba_{1.3}Sr_{1.7}MgSi_2O_8:Eu^{2+}$, Mn^{2+} phosphor convertor doesn't meet the applicable requirement of high-power LEDs.

Inspired by the previous progress, in this work, a high power light converting device with blue and red dual-broadband emission was reported, which is prepared by PiG approach, improving the service life and solving the problem of light leakage, composing of the glass matrix embedding the $Ba_{1.3}Sr_{1.7}MgSi_2O_8:Eu^{2+},Mn^{2+}$ phosphors. The microstructure, luminescent properties and thermal stability of BSMS-PiG had been meticulously investigated. These results agree with the analysis of Deng et al and Li et al, in that the photoluminescence (PL) of BSMS phosphor can be well maintained in PiG and the thermal stability of BSMS -PiG is better than that of phosphor. Furthermore, in order to adapt to the growth needs of various plants, the red-blue ratio of BSMS-PiG based on ~370 nm LED chip was regulated by controlling the thickness of BSMS-PiG and the concentrations of Mn^{2+} ions in BSMS-PiG. Meanwhile, the 7 wt% BSMS-PiG plates were applied in high-power horticultural LEDs to improve the Romaine lettuce growth.

2 Experimental

2.1 Phosphor preparation

Phosphor samples of an optimized nominal composition in $Ba_{1.3}Sr_{1.7}MgSi_2O_8$: 6% Eu^{2+}, x% Mn^{2+} with x = 1, 2, 3, 4, 5 and 6 were prepared by a conventional solid reaction method. The reagents were $BaCO_3$(99.9%, Aladdin), $SrCO_3$(99.9%, Aladdin), MgO(99.9%, Aladdin), SiO_2(99.9%, Aladdin), Eu_2O_3(99.9%, Aladdin) and $MnCO_3$(99.9%, Aladdin). The six raw materials were mixed entirely with fluxing agent (5% of NH_4Cl) and a suitable amount of ethanol at agate mortar and then dried at 80 °C for 1 h. Then the mixture was sintered in corundum crucibles at 1250 °C for 8 h under a reducing gas atmosphere (5% H_2-95% N_2). Finally, the naturally cooled samples were grinded to a fine powder for fluorescent component of PiG.

2.2 Light convertor synthesis

Precursor glasses with following compositions (mol%) of $38SiO_2$-$10B_2O_3$-12ZnO-$15Na_2O$-$5K_2O$-$5Al_2O_3$-15CaO were prepared. The mixed raw materials were heated at 1350 °C for 1 h in a corundum crucible. After cooling, the glass was milled into glass frits. The relative ratio of the BSMS phosphor to glass matrix was fixed at the range of 1~7 wt%. A series of BSMS-PiG were prepared by mixing phosphor particle and the glass frit in an agate mortar, and then the mixture powder were sintered at 585 °C for 1 h with a reducing gas atmosphere (5% H_2-95% N_2) after being compressed into sheets under 30 MPa pressure. Moreover, the phosphor-in-silicone (PiS) was synthesized by dispersing the BSMS phosphor in organic silicone (purchased from DC184 silicone of Dow Corning).

2.3 Plant cultivation

Indoor Romaine lettuce cultivation experiments were conducted by hydroponics under different photosource including BSMS-PiG based LEDs with ~370 chip and the reference commercial plant lamps (Model JL-2835-60W, Dongguan Longfar Optoelectronics Technology Co., Ltd.). All Romaine lettuce samples at seedling growth stage were initially cultivated under identical illumination conditions and environment for 14 days and then transplanted into indoor to be adopt light treatments (intensity at 80~100 $\mu mol \bullet m^{-2} \bullet s^{-1}$ photosynthetic photon flux density) in several by these two plant growth LEDs above-mentioned for 7 days. The environmental temperature is 22±3 °C, the humidity is ~(60~65%), and the carbon dioxide concentration is 340±20 ppm. The indicators of shoot weigh (fresh and dry) were measured and the data of 4 random plant averaged, while the rest of indicators are obtained for 4 times. All indicators are gauged according to previously disclosed methods[27,28].

2.4 Characterizations

Powder X-ray diffraction (XRD) was performed on Bruker Ultima-IV X-ray diffractometer with Cu Kα (λ=1.5405 Å) radiation at 40 kV and 40 mA. The morphology and elemental composition were measured by scanning electron microscope (SEM), equipped with an energy dispersive spectroscopy (EDS) system (Hitachi SU8220, Japan). Laser scanning microscopy (LSM) images were collected with a confocal laser scanning microscope (DM6000 B, LEICA), equipped with a 405 nm laser as an excitation source. The photoluminescence excitation (PLE) and photoluminescence emission (PL) spectra in the temperature range: 298-478 K were measured using F-7000 Fluorescence Spectrometers (Hitachi, Ltd., Japan) equipped with a 150 W xenon lamp as an excitation source. The quantum efficiency and absorption efficiency were measured by FLS1000 (Edinburgh Instruments, Britain). The heat transfer phenomena of the BSMS-PiG and BSMS-PiS based on LED chip with 1 A current were studied using a FLIR E40 infrared camera (FLIR System, Inc., United States). The irradiance of high-power horticultural LEDs were measured by TA8123 digital light meter (Suzhou TASI Electronics Co., Ltd., China).

3 Results and discussion

In order to inspect the possible reaction between the phosphor and glass, SEM, EDS, and EDS mapping were carried out. Exhibited in Fig. 1a, it is clearly seen that the BSMS phosphor particles were embedded in the glass matrix. The elements including Na, Zn, Sr, Ba and Mg are distributed quite homogeneous in the EDS mapping images of BSMS-PiG. The Na- and Zn-rich regions represent the glass matrix, while the Sr-, Ba- and Mg-rich portions demonstrate the phosphor particles. Based on these characterizations of SEM and EDS mapping, all those results indicates that the BSMS phosphor particles are integrated as the powder in the glass matrix.

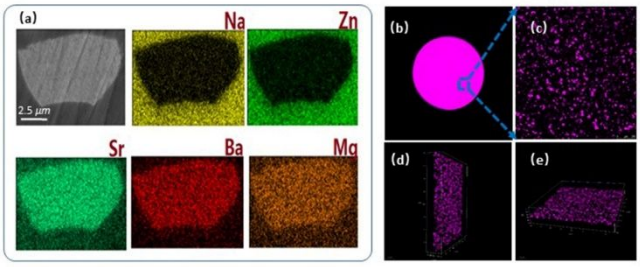

Fig. 1 (a) SEM image of 7 wt% BSMS-PiG, and SEM mappings of the elementals correspond to BSMS phosphor and glass matrix. (b) Photograph of 7 wt % BSMS-PiG sample under 365nm UV light; (c) Surface fluorescence distribution image; and (d,e) 3D reconstruction images of 7 wt % BSMS-PiG sample.

To clearly watch the distribution of BSMS phosphor powder inside the glass matrix, confocal laser scanning microscope (CLSM) was employed with a laser wavelength of 405 nm. Exhibited in Fig. 1b, pink emission can be observed in PiG under 365 nm UV light, determining initially that the BSMS phosphor has been integrated into glass matrix. The horizontal fluorescence distribution of BSMS phosphor particles inside PiG is clearly shown in Fig. 1c. The pink lightspots indicate phosphor particles, while the rest of the area represents glass matrix. Based on the above results, a conclusion can be drawn that the BSMS phosphor particles are uniformly dispersed in the glass matrix. Moreover, uniform spatial distribution of 7 wt% BSMS phosphor in PiG were also shown in Fig. 1d-e to illustrate the well distribution of phosphor particles in the PiG sample.

The photoluminescence excitation (PLE) and photoluminescence (PL) spectra of BSMS-PiG and the corresponding BSMS phosphor powder are shown in Fig. 2a. Excitation spectrum exhibit band emission ranging from UV to NUV with the main peak around 355 nm (owing to 4f-5d transition of Eu^{2+}). The PL spectrum of BSMS-PiG and BSMS phosphor displays dual-emitting, consisting of 430 nm-blue emission band arising from the electric-dipole allowed $4f^65d^1 \rightarrow 4f^7$ transition of Eu^{2+} ions and 660 nm-red emission band resulting from the $^4T(^4G) \rightarrow {}^6A_1(^6S)$ transition of $3d^5$ energy level of Mn^{2+} ions[29]. The luminescent properties of BSMS-PiG and BSMS phosphor are similar to each other both on the excitation and emission bands in location.

All the BSMS-PiG&BSMS samples have the similar decay curve configuration because of the representative $4f^65d^1 \rightarrow 4f^7$ electric-dipole transition of Eu^{2+}. As demonstrated in Fig. 2b, these decay curves were well fitted with a typical single exponential function, and the Eu^{2+} lifetime of 7 wt% BSMS-PiG was determined to be about 218.09 ns, which is close to the case of the 212.69 ns of the Eu^{2+} lifetime of BSMS phosphor. These results prove that the fluorescent lifetime isn't affected by the glass matrix.

In Fig. 2c, the PL intensity of BSMS-PiG can be improved by increasing the phosphor doping concentration, and the maximum value appears at 7.0%. The internal quantum efficiency (IQE), external quantum efficiency (EQE) and absorption efficiency (AE) of BSMS-PiG and BSMS phosphor were measured under 365 nm excitation in 25 °C for further proving practical application of BSMS-PiG. As described in Fig. 2d, this overall trend of BSMS-PiG samples is upward with the phosphor doping concentration increases, of which the maximum value of IQE reveal at 5 wt% BSMS-PiG and the maximum value of AE and EQE present at 7 wt% BSMS-PiG. But compared with BSMS phosphor (EQE = 57.54%), the EQE of BSMS-PiG is dramatic decline. This phenomenon has been summarized in numerous articles[30-32] but this part of efficiency loss is acceptable to improve the chemical stability of BSMS phosphor. Therefore, combining the above results, it can be seen that 7 wt% BSMS-PiG is a great selection for high-power plant lighting.

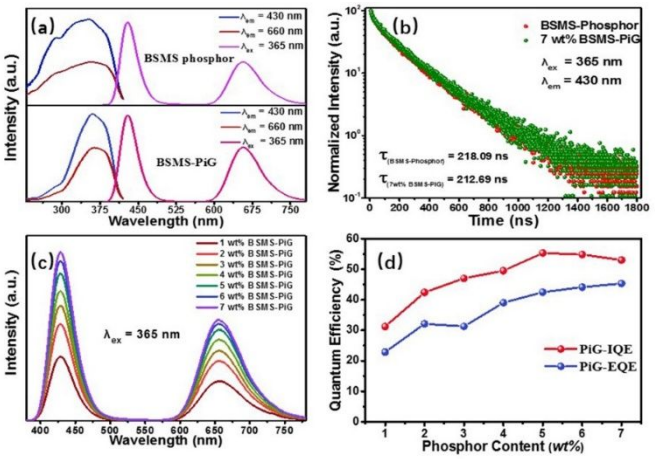

Fig. 2 (a) PLE, PL spectra and (b) luminescence decay curves of BSMS phosphor and 7 wt% BSMS-PiG. (c) PL and (d) quantum efficiency of BSMS-PiG with different phosphor doping concentrations.

It is widely acknowledged that the thermal stability of luminescence is a significant argument to assess the application of luminescent materials in high-power LED devices. In this perspective, the temperature dependent luminescent emission spectra of the 7 wt% BSMS-PiG and phosphor sample were measured. As shown in Fig. 3a and b, the Eu^{2+} emission bands (380−500 nm) manifest an apparent thermal quenching but the emission intensity of Mn^{2+} emission bands (580−780 nm) increases with the temperature increases under 365 nm excitation. What needs to be mentioned here is the anti-Stokes effect[33]. Generally, emission intensity of fluorescence spectrum is defined as follows[34]:

$$I \propto ANhv$$

Where *I* is the emission spectrum intensity, *A* is the autonomous transition probability, *N* is the electron population, *h* is the Planck constant, and *v* is the emitting light frequency. The electron population in the vibrational ground state dwindle down with temperature increasing. On the contrary, the electron population in the vibrational excitation states rise up. Accordingly, the emission intensity of anti-Stokes emission region will increase and the intrinsic temperature quenching effect of the material can be partially

compensated just as the phenomenon of Mn^{2+} emission bands (550−780 nm) with rising temperature. The thermal quenching of 7 wt% BSMS-PiG is less influenced by temperature in comparison with BSMS phosphor. Furthermore, the intensity of anti-Stokes emission bands in 7 wt% BSMS-PiG demonstrates much more temperature dependent than that in BSMS-phosphor, because the anti-Stokes effect prevails over the thermal quenching effect. As shown in Fig. 3c, the normalized intensity of BSMS phosphor and 7 wt% BSMS-PiG in the blue emission region is respectively reduced to 0.626 and 0.784 especially at 475 K, and the normalized intensity of BSMS phosphor and 7 wt% BSMS-PiG in the red emission region is respectively increased by 16.6% and 34.8%, compared to 298 K. For many plants, red light promotes the growth of stem, leaf and fruit more than blue light during the plant growth cycle. Therefore, the anti-Stokes effect of BSMS-PiG is just suitable for the application of high-power lamps for plant growing.

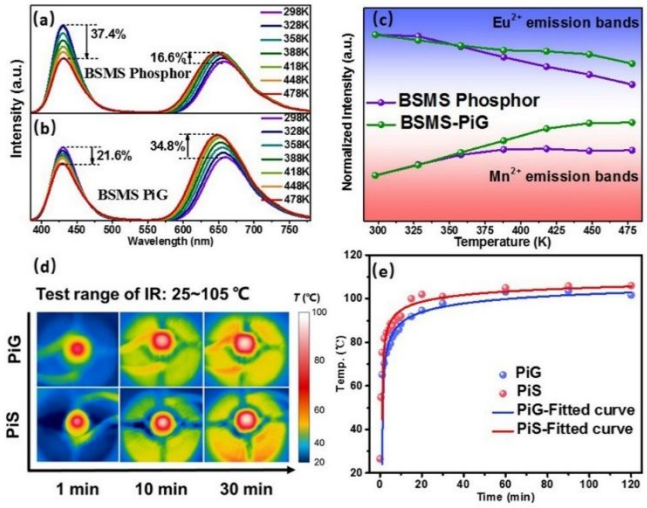

Fig. 3 Temperature-dependent emission spectra of (a) BSMS phosphor and (b) 7 wt% BSMS-PiG recorded from 298 to 478 K. (c) The variation of corresponding normalized intensity in BSMS phosphor and 7 wt% BSMS-PiG. (d) The thermal images of BSMS-PiG and BSMS-PiS based on LED chip with 1A current under different operating times, and (e) temperature as a function of the time of operation.

In addition, the thermal transfer phenomena were evaluated by thermographic images that emerged the concentric distribution of thermal energy on the surface of the BSMS-PiG and BSMS-PiS as described in Fig. 3d. The BSMS-PiG show a broader radial temperature gradient zone. The increase in the area over which thermal energy has spread makes the convection process more effective. The temperatures as a function of time were plotted in Fig. 3e. The surface temperature has a dramatic rise when the LED chip was turn on, and then up to a maximum of 100 °C after 30 min. The BSMS-PiG showed 3.1~11.2% lower temperatures at surfaces compared with the BSMS-PiS. There is the reason for this phenomenon that the BSMS-PiG has a higher thermal conductivity (~1.242 $W•m^{-1}•K^{-1}$), which is superior to the BSMS-PiS (thermal conductivity ~0.16 $W•m^{-1}•K^{-1}$) and contributes the heat spreading. That can be in favour of weakening the thermal quenching of the embedded BSMS phosphor.

The energy required for plant growth and morphogenesis is mainly provided by light energy, especially in blue-, red-, and far red-light. The spectrum of BSMS-PiG exactly matches the absorption of plant pigments. Therefore, it was used to assemble the plant lights as shown in Fig. 4a and b. However, the wavelength of light required for the growth of different plants is also different[35], thus it is of great significance to regulate the ratio of blue light and red light for the growth of different plants. Here, the PL spectra of different thickness of 7 wt% BSMS-PiG and different concentrations of Mn^{2+} ions in BSMS-PiG based on ~370 nm chip were determined, and the PL spectra with different red-blue ratios as exhibited in fig. 4c and d. The proportion of blue light decreases while the proportion of red light increases and the overall luminescence intensity decreases with the thickness of BSMS-PiG increasing. As the propagation path of light in the glass gets longer, blue light is absorbed by phosphor to excite red light, thus changing the ratio of blue to red. In addition, the effect of changing thickness on absorptivity (abs.) and conversion efficiency (η_c) of 7 wt% BSMS-PiG was exhibited in Fig. 4e, and calculated according to the following equations:

$$\text{abs.} = \frac{\int [Ex(\lambda) - T(\lambda)] d\lambda}{\int Ex(\lambda) d\lambda}$$

$$\eta_c = \frac{\int Em(\lambda) d\lambda}{\int [Ex(\lambda) - T(\lambda)] d\lambda}$$

Where $Ex(\lambda)$,$Em(\lambda)$ and $T(\lambda)$ are the intensities per unit wavelength in excitation, emission and transmitted light spectra of BSMS-PiG. The absorption of ultraviolet light by glass substrate increases because of the increasing of the thickness of BSMS-PiG so that the phosphors in the glass cannot be completely excited, that result in the overall luminescence intensity shows a downward trend. It is well understood that the red-blue ratio can be adjusted by reasonably increasing the concentration of phosphor doped Mn^{2+} ions at the same condition. The luminescent lifetime of Eu^{2+} ion decreases gradually (Fig. 4f) when the concentration of Mn^{2+} increases from 1 to 6 mol%. This is mainly due to the increasing of luminescence of Mn^{2+} ions and the energy transfer between Eu^{2+} and Mn^{2+}[36].This is mainly due to the increasing of luminescence of Mn^{2+} ions and the energy transfer between Eu^{2+} and Mn^{2+}. As the concentration of Mn^{2+} increases from 1 to 6 mol%, the PL intensity of Eu^{2+} decreases monotonically, whereas that the PL intensity of Mn^{2+} is increasing. The PL intensity ratio of blue to red is around 1:0.3 to 1:3.5.

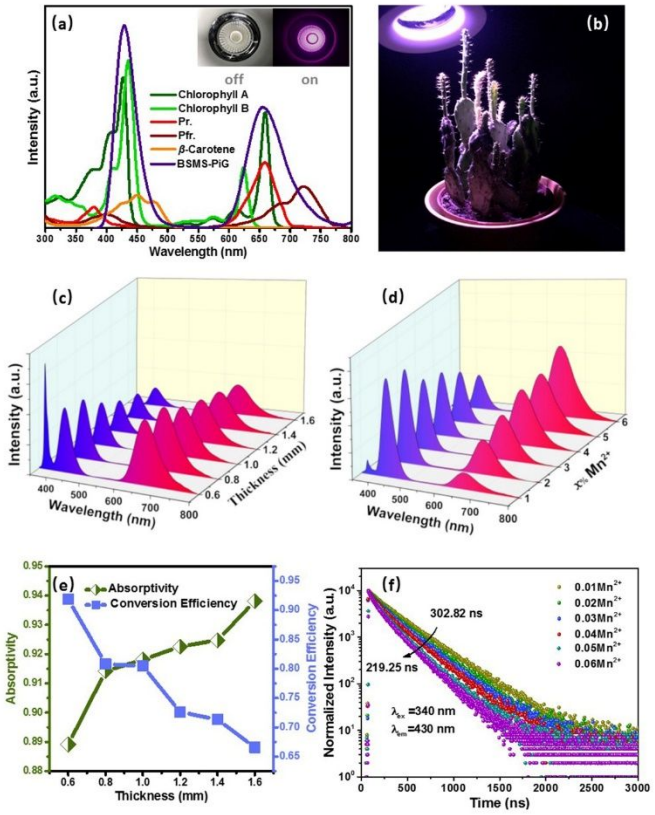

Fig. 4 (a) Plant photosynthesis absorption spectrum and EL spectrum of 7 wt% BSMS-PiG base on ~370 nm LED chip. (b) Plant lamp concept schematic. Spectra of different blue-red ratios of BSMS-PiG plant lamps (c) with 7 wt% doping phosphor concentrations at various thicknesses, and (d) with different concentrations of Mn^{2+} dope BSMS phosphors at the thickness of 1.0 mm. (e) The effect of changing thickness on absorptivity and conversion efficiency of 7 wt% BSMS-PiG. (f) Luminescence decay curves of 7 wt% $Ba_{1.3}Sr_{1.64}Mg_{1-x}Si_2O_8$:0.06$Eu^{2+}$, x$Mn^{2+}$-PiG on 430nm.

Finally, the influence of light treatment on Romaine lettuce growth were carried out using the 7 wt% BSMS-PiG plant lamp, and the commercial plant lamp was the reference, manifested in Fig. 5a. The middle part of the planting area was used as a reasonable sample selection area to ensure the evenness of illumination and the reliability of experiment. The emission spectra of these two kinds of horticultural LEDs demonstrate in Fig. 5b, in which the BSMS-PiG plant lamp has almost the same emission peak as the commercial plant growth LEDs, but the full width at half-maximum of the former (~44 nm in blue region, 79 nm in red region) is obviously wider than that of the latter (~25 nm in blue region, 24 nm in red region). The facilitation of them in cultivating Romaine lettuce is distinguishing. After being cultivated for 3 weeks, the Romaine lettuce which take in the light treatment with BSMS-PiG based on ~370 nm chip have greener and bigger leaves than that with the commercial plant lamp, presenting in Fig. 5c, and the comparison of single between the sample group A and B can be more clearly seen. In addition, to further a detailed verification, parameters for biomass of plant were listed in Table 1 including quality index, chlorophyll content, β-carotene content and soluble protein content. Samples-A under the irradiation with BSMS-PiG horticultural LEDs have better physiological index than Samples-B under the irradiation with the commercial plant lamp, increase by 62.58% for fresh weight, 58.27% for dry weight, 26.05% for total chlorophyll content, 22.82% for β-carotene content and 21.40% for soluble protein content, respectively. The results of the indoor cultivation experiment of Romaine lettuce indicate that the BSMS-PiG horticultural LEDs is a superior light source for facilitating plant growth, increasing crop, accelerating product morphology and boosting nutrient substance. Consequently, the BSMS-PiG horticultural LEDs with brilliant spectral characters is a potential candidate for high power horticultural light source to substitute for conventional plant lamp.

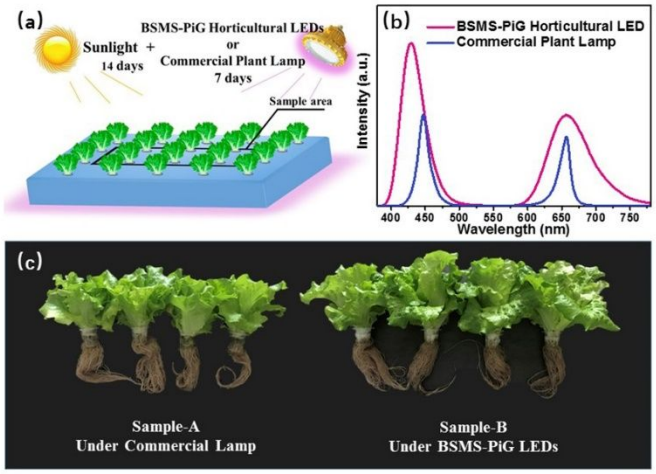

Fig. 5 (a) Abridged general view of Romaine lettuce cultivation irradiated by different light sources. (b) EL spectra of BSMS-PiG horticultural LED and the commercial plant lamp. (c) Photograph of Romaine lettuce cultivation under different light treatments.

Table 1. Effect of different light on the indicators of Romaine lettuce samples.

	Fresh weight (g•plant^{-1})	Dry weight (g•plant^{-1})	Total chlorophyll content (mg•g^{-1})	β-carotene content (mg•g^{-1})	Soluble protein content (mg•g^{-1})
A	26.224	1.215	0.787	0.149	2.051
B	42.636	1.923	0.992	0.183	2.490

4 Conclusions

In summary, the $Ba_{1.3}Sr_{1.7}MgSi_2O_8$:$Eu^{2+}$,$Mn^{2+}$ phosphors with bright broadband dual-emitting were synthesized by conventional high temperature solid-state method, and the phosphor was further developed as a stable light converter thought phosphor-in-glass approach for high-power horticultural LEDs. The BSMS-PiG sustains the luminescent properties of BSMS phosphor and the high extern quantum efficiency of 45.3%. Compared to BSMS phosphor, BSMS-PiG exhibits better thermal stability in the temperature range of 298 to 478 K. Not only that, but the BSMS-PiG shows a superior thermal conductivity (~1.242 W•m^{-1}•K^{-1}) which contributes the heat spreading to impair the thermal quenching of the embedded BSMS phosphor. Furthermore, the blue-red ratio of

intensity of BSMS-PiG plant lamp was adapted to the growth of different plants by controlling thickness of BSMS-PiG and concentrations of Mn^{2+} ions in BSMS-PiG base on ~370 nm chip. The results of the indoor cultivation experiment of Romaine lettuce indicate that the BSMS-PiG with brilliant spectral characters and superior thermal stability is an ideal candidate light convertor for high-power horticultural LEDs.

Acknowledgements

The present work was supported by the National Natural Science Foundations of China (Grant No. 21671070); the Project of GDUPS (2018) for Prof. Bingfu LEI; the Guangzhou Science & Technology Project, China (No. 201704030086); and the National Undergraduate Innovation and Entrepreneurship Training Program granted for Gening Xie (No. 201910564035).

Notes and references

1 J. Zhan, I. Twardowska, S. Wang, S. Wei, Y. Chen and M. Ljupco, *Journal of Cleaner Production*, 2019, **212**, 22-36.

2 J. D. B. Gil, P. Reidsma, K. Giller, L. Todman, A. Whitmore and M. van Ittersum, *Ambio*, 2019, **48**, 685-698.

3 C. A. Mitchell, in *Vii International Symposium on Light in Horticultural Systems*, eds. S. Hemming and E. Heuvelink, 2012, **956**, 23-36.

4 M. Olle and A. Virsile, *Agricultural and Food Science*, 2013, **22**, 223-234.

5 M. Xia, X. Wu, Y. Zhong, Z. Zhou and W.-Y. Wong, *Journal of Materials Chemistry C*, 2019, **7**, 2385-2393.

6 R. Dong, Y. Li, W. Li, H. Zhang, Y. Liu, L. Ma, X. Wang and B. Lei, *Journal of Rare Earths*, 2019, DOI: 10.1016/j.jre.2019.04.001.

7 C. M. Bourget, *HortScience*, 2008, **43**, 1944-1946.

8 Z. Xia and Q. Liu, *Progress in Materials Science*, 2016, **84**, 59-117.

9 N. Yeh and J.-P. Chung, *Renewable and Sustainable Energy Reviews*, 2009, **13**, 2175-2180.

10 E. Darko, P. Heydarizadeh, B. Schoefs and M. R. Sabzalian, *Philos Trans R Soc Lond B Biol Sci*, 2014, **369**, 20130243.

11 M. H. Chang, D. Das, P. V. Varde and M. Pecht, *Microelectronics Reliability*, 2012, **52**, 762-782.

12 R. Zhang, H. Lin, Y. Yu, D. Chen, J. Xu and Y. Wang, *Laser & Photonics Reviews*, 2014, **8**, 158-164.

13 S. Nishiura, S. Tanabe, K. Fujioka and Y. Fujimoto, *Optical Materials*, 2011, **33**, 688-691.

14 N. Wei, T. Lu, F. Li, W. Zhang, B. Ma, Z. Lu and J. Qi, *Applied Physics Letters*, 2012, **101**, 061902.

15 D. Chen, Y. Zhou, W. Xu, J. Zhong, Z. Ji and W. Xiang, *Journal of Materials Chemistry C*, 2016, **4**, 1704-1712.

16 B. Wang, H. Lin, F. Huang, J. Xu, H. Chen, Z. Lin and Y. Wang, *Chemistry of Materials*, 2016, **28**, 3515-3524.

17 J. Deng, H. Zhang, X. Zhang, Y. Zheng, J. Yuan, H. Liu, Y. Liu, B. Lei and J. Qiu, *Journal of Materials Chemistry C*, 2018, **6**, 1738-1745.

18 M. Li, X. Zhang, H. Zhang, W. Chen, L. Ma, X. Wang, Y. Liu and B. Lei, *Journal of Materials Chemistry C*, 2019, **7**, 3617-3622.

19 S. M. Zahedi and H. Sarikhani, *Russian Journal of Plant Physiology*, 2017, **64**, 83-90.

20 S. Oh and B. L. Montgomery, *Cell*, 2017, **171**, 1254-1256.

21 E. Kim, S. Unithrattil, I. S. Sohn, S. J. Kim, W. J. Chung and W. B. Im, *Optical Materials Express*, 2016, **6**, 255933.

22 J. He, L. Qin, E. L. Chong, T. W. Choong and S. K. Lee, *Front Plant Sci*, 2017, **8**, 361.

23 L. Cao, Q. Lu, L. Wang, J. Li, J. Song and D. Wang, *Ceramics International*, 2013, **39**, 7717-7720.

24 J. K. Han, A. Piqutte, M. E. Hannah, G. A. Hirata, J. B. Talbot, K. C. Mishra and J. McKittrick, *Journal of Luminescence*, 2014, **148**, 1-5.

25 L. Sun, Q. Lu, Z. Mao and D. Wang, *Journal of Materials Science: Materials in Electronics*, 2015, **26**, 2647-2653.

26 Z. Mao, J. Chen, L. Sun, Q. Lu and D. Wang, Materials Research Bulletin, 2015, 70, 908-913.

27 J. Zhang, L. Dong and S.-H. Yu, *Science Bulletin*, 2015, **60**, 785-791.

28 Y. Zheng, G. Xie, X. Zhang, Z. Chen, Y. Cai, W. Yu, H. Liu, J. Shan, R. Li, Y. Liu and B. Lei, *ACS Omega*, 2017, **2**, 3958-3965.

29 Z. Tian, Y. Qiu and J. Cai, *Ceramics International*, 2016, **42**, 6369-6374.

30 H. Segawa, S. Ogata, N. Hirosaki, S. Inoue, T. Shimizu, M. Tansho, S. Ohki and K. Deguchi, *Optical Materials*, 2010, **33**, 170-175.

31 H. Lin, T. Hu, Y. Cheng, M. Chen and Y. Wang, *Laser & Photonics Reviews*, 2018, **12**, 1700344.

32 M. Li, H. Zhang, X. Zhang, J. Deng, Y. Liu, Z. Xia and B. Lei, *Materials Research Bulletin*, 2018, **108**, 226-233.

33 J. Chen, W. Zhao, N. Wang, Y. Meng, S. Yi, J. He and X. Zhang, *Journal of Materials Science*, 2016, **51**, 4201-4212.

34 R. N. Zare, *The Journal of Chemical Physics*, 1964, **40**, 1934-1944.

35 S. Dutta Gupta and B. Jatothu, *Plant Biotechnology Reports*, 2013, **7**, 211-220.

36 Y. Sun, P. Li, Z. Wang, J. Cheng, Z. Li, C. Wang, M. Tian and Z. Yang, The Journal of Physical Chemistry C, 2016, 120, 20254-20266.

A Glass-ceramics with Thermally Stable Blue-red emission for High-power Horticultural LEDs Application

Weibin Chen,[a] Xuejie Zhang,[a] Jianxian Zhou,[a] Haoran Zhang,[a] Xiang Yang,[b] Zhiguo Xia,[c] Yingliang Liu,[a] Maxim S. Molokeev,[d,e] Gening Xie,[1] and Bingfu Lei[a,b,*]

[a]*Guangdong Provincial Engineering Technology Research Center for Optical Agriculture, College of Materials and Energy, South China Agricultural University, Guangzhou 510642, P. R. China*

[b]*College of Horticulture, South China Agricultural University, Guangzhou 510642, P. R. China*

[c]*The State Key Laboratory of Luminescent Materials and Devices, and Guangdong Provincial Key Laboratory of Fiber Laser Materials and Applied Techniques, School of Materials Science and Engineering, South China University of Technology, Guangzhou 510641, P. R. China4*

[d]*Laboratory of Crystal Physics, Kirensky Institute of Physics, Federal Research Center KSC SB RAS, Krasnoyarsk 660036, Russia*

[e]*Siberian Federal University, Krasnoyarsk 660041, Russia*

**tleibf@scau.edu.cn*

Supplementary materials

Table S1. Main parameters of processing and refinement of the $Sr_{1.7-x}Ba_{1.3}Eu_xMg_{1-y}Mn_ySi_2O_8$ sample.

Compound	$Sr_{1.7}Ba_{1.3}MgSi_2O_8$	$Sr_{1.64}Ba_{1.3}Mg_{0.94}Si_2O_8$: 6%$Eu^{2+}$, 6%$Mn^{2+}$
Sp.Gr.	*P*-3*m*1	*P*-3*m*1
a, Å	5.50301 (13)	5.5194 (2)
c, Å	7.02584 (17)	7.0536 (3)
V, Å^3	184.26 (1)	186.09 (2)
2θ-interval, º	8-111	8-120
R_{wp}, %	8.25	5.84
R_p, %	6.00	4.40
R_{exp}, %	3.12	3.02
χ^2	2.64	1.94
R_B, %	5.66	5.16

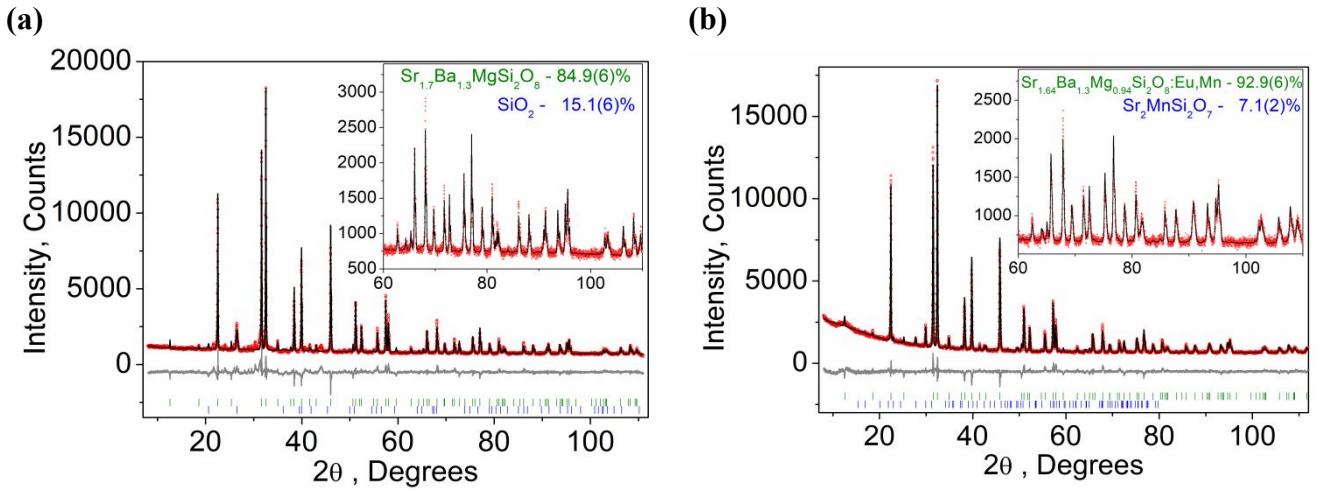

Fig. S1 Difference Rietveld plot of: (a) $Sr_{1.7}Ba_{1.3}MgSi_2O_8$; (b) $Sr_{1.64}Ba_{1.3}Eu_{0.06}Mg_{0.94}Mn_{0.06}Si_2O_8$.

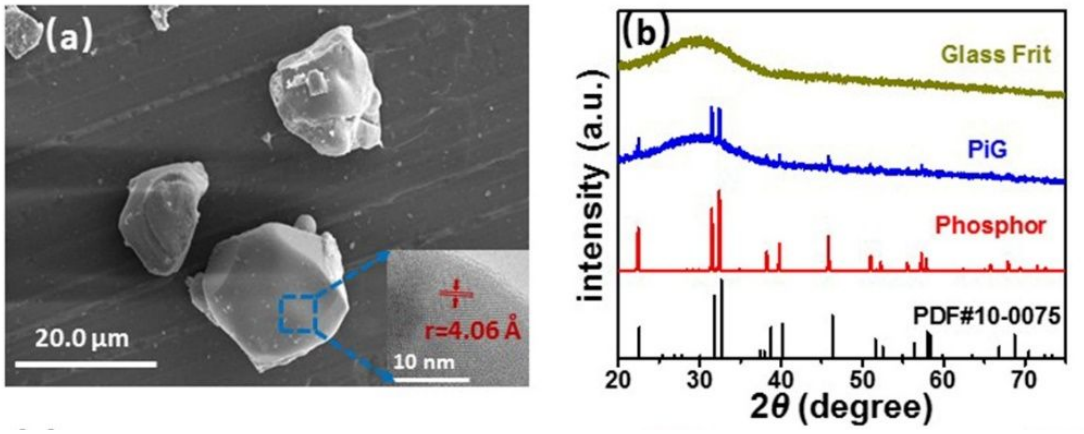

Fig. S2. (a) SEM and HRTEM images of BSMS phosphor. (b)XRD patterns of BSMS phosphor, glass frit, 7 wt% BSMS-PiG and standard data of $Sr_3MgSi_2O_8$ (PDF#10-0075).

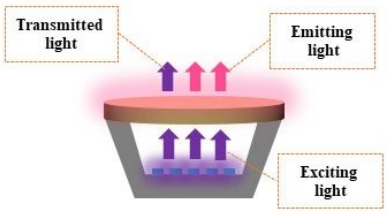

$$abs. = \frac{\int [Ex(\lambda) - T(\lambda)]d\lambda}{\int Ex(\lambda)d\lambda}$$

$$\eta_c = \frac{\int Em(\lambda)d\lambda}{\int [Ex(\lambda) - T(\lambda)]d\lambda}$$

$Ex(\lambda)$ —— Intensity per unit wavelength in exciting light
$Em(\lambda)$ ——Intensity per unit wavelength in emitting light
$T(\lambda)$ —— Intensity per unit wavelength in transmitted light of UV

Fig. S3 Schematic of absorption and conversion efficiency

The measurement of photosynthetic pigment contents

0.5g of fresh lettuce leaves were immersed in 25mL organic solvent (acetone : ethyl alcohol = 1 : 1 in Vol%) for 24h. The supernatant was measured at 645 nm, 663 nm and 440 nm. Equations for

calculating were following:

$$Total\ chlorophyll\ content\ \left(mg \bullet L^{-1}\right) = 8.02 \times OD_{663} + 20.20 \times OD_{645}$$

$$\beta - carotene\ content\ \left(mg \bullet L^{-1}\right) = 4.7 \times OD_{440} - 0.27 \times \left(8.02 \times OD_{663} + 20.20 \times OD_{645}\right)$$

$$\text{Pigment content}\ \left(mg \bullet \text{g}^{-1}\right) = \frac{\text{Pigment content}\ \left(mg \bullet L^{-1}\right) \times V}{W}$$

OD is the absorbance at 645 nm, 663 nm and 440 nm; *V* is the volume of extraction liquid; *W* is the weight of fresh lettuce leaves.

The measurement of soluble protein

The 1.0 g of lettuce sample was shaken with 8 mL deionized water in a centrifuge tube, and centrifuged at 3000rpm for 10 min. 0.2 mL of the supernatant was collected, then added with 0.8 mL deionized water and 5 mL of Coomassie brilliant blue G–250. After 5 min, the above liquor was measured at 595 nm, using bovine serum albumin as protein standard.